S. A. Veress
Department of Civil Engineering
University of Washington
Seattle, WA 98195
J. N. Hatzopoulos
California State University at Fresno
Fresno, CA 93740

A Combination of Aerial and Terrestrial Photogrammetry for Monitoring

The accuracy of this combined approach is considerably better than that of the terrestrial photogrammetric process alone.

Abstract: *Research conducted for investigating the methodology and feasibility of combining aerial and terrestrial photogrammetry is described in detail. The formulation of mathematics designed for medium sized computers are presented.*

The geometry of this combination was first tested on a simulated terrain model. The testing of the model indicated the design limitations and advantages. A practical test of the method was then performed on a retaining wall. The final results indicated the feasibility of the method as well as its flexibility. The accuracy of this combined approach is considerably better than that of the terrestrial photogrammetric process alone.

Introduction

The existing application of photogrammetry for structural deformation or motion measurement is strictly limited to either terrestrial or aerial photography. There are, however, structure and terrain combinations where these applications are suffering from topographic restrictions. A method combining aerial and terrestrial photographs would free the photogrammetric application from restrictions, thus, allowing the practitioner to obtain the optimum geometry of the monitoring system even when the terrain features do not permit favorable locations of the terrestrial camera platform or the complete structure could not be imaged on aerial photographs.

The Washington Department of Transportation, in cooperation with the Federal Highway Administration, sponsored research projects in 1968 and 1975 to develop analytical photogrammetric methods to monitor structural deformations (Veress, 1971; Veress and DeGross, 1971; Veress *et al.*, 1973). These projects utilized terrestial photographs with various analytical approaches. The general design, geometrical difficulties, and the desire to achieve a higher degree of accuracy lead to a research project in 1977 to utilize the combination of aerial and terrestrial photographs (Veress and Hatzopoulos, 1979).

The mathematical approach applied in photogrammetric monitoring consists of sequential photogrammetric adjustment, as reported in current literatures (Planicka, 1970; Veress, 1971; Brandenberger and Erez, 1972; Guto, 1972; Hou, 1979; Veress and Sun, 1978). These studies are based on the computational elements of classical aerial triangulation. Relatively few applications are based on a rigorous simultaneous adjustment method (Kenefick, 1971; Erlandson and Veress, 1975; Veress et al., 1973) because the simultaneous adjustment of bundle method requires a large computer core storage memory.

Photogrammetric Engineering and Remote Sensing,
Vol. 47, No. 12, December 1981, pp. 1725-1731.
0099-1112/81/4712-1725$02.25/0

In this research project, both sequential and simultaneous adjustments are utilized and the results are analyzed. One of the objectives of this study is to use a small computer core storage memory (less than 77K in the University of Washington Cyber 73/CDC 6400 computer) and a small amount of computer time.

MATHEMATICAL CONCEPT

There are two forms of mathematical treatment of the problem. One is a sequential solution and the other is a simultaneous adjustment.

The sequential adjustment is performed in several steps according to a particular order. The sequential steps are

- *Refinement of plate coordinates.* Corrections for film distortion, and comparator errors, lens distortion, and atmospheric refraction, and reduction to the principal point.
- *Space resection.* Coordinates of the front nodal point of the camera are determined by space resection. This particular mathematical process is described by Erlandson and Veress (1975) and Veress (1980) for space resection, the orientation matrix, and space intersection.
- *Determination of the orientation matrix.* The orientation matrix is determined separately and the process is not iterative, which is the case with other solutions.
- *Space intersection.* The intersection coordinates of two or more rays, which correspond to the same object point imaged in two or more photographs, are obtained by a least-squares adjustment. The standard error of these coordinates are obtained from space intersection computations only; thus, the sequential adjustment is not a rigorous mathematical solution.

The sequential adjustment is also capable of providing the a priori values of parameters for the simultaneous adjustment.

The sequential adjustment is advantageous from a computational point of view, but its general implication fails to incorporate the full mathematical foundation of a simultaneous adjustment, which yields the most accurate results and which in turn lends itself to statistical assessment with respect to a posteriori precision evaluation and gross error detection.

There are several approaches to the performance of a simultaneous adjustment. Schmid (1956) used the coplanarity conditions, Brown (1974, 1976) used the collinearity conditions in the bundle method, and Veress (1973) used a collinearity equation in connection with geodetic measurements. There are a number of other approaches such as the use of tensor analysis, complex numbers, etc. Here, the collinearity condition will be used in a similar manner as it is used in the bundle adjustment with special emphasis on minimum computer storage requirements.

Assuming that the j^{th} ground point is imaged on the i^{th} photograph, the collinearity equations can be expressed as

$$x_{ij} = -f\frac{(X_j - X_i)m_{11} + (Y_j - Y_i)m_{12} + (Z_j - Z_i)m_{13}}{(X_j - X_i)m_{31} + (Y_j - Y_i)m_{32} + (Z_j - Z_i)m_{33}}$$

$$y_{ij} = -f\frac{(X_j - X_i)m_{21} + (Y_j - Y_i)m_{22} + (Z_j - Z_i)m_{33}}{(X_j - X_i)m_{31} + (Y_j - Y_i)m_{32} + (Z_j - Z_i)m_{33}}$$

where x_{ij}, y_{ij} are the measured photo-coordinates; $X_j\ Y_j\ Z_j$ are the ground coordinates of j^{th} point; $X_i\ Y_i\ Z_i$ are coordinates of the i^{th} camera station; f is the focal length of the camera; and $m_{ij}(i = 1, 2, 3; j = 1, 2, 3)$ are the elements of the orientation matrix of the i^{th} photograph.

The above equations may be noted in the form of functions i.e.,

$$x_{ij} = F \text{ and } y_{ij} = G.$$

A complete mathematical model of all the optical rays in pair of photographs can be constructed by using collinearity equations for every object point. The parameters of this model are the elements of orientation matrix as a function of the ω, ϕ, κ, rotational angles and the $X_i\ Y_i\ Z_i$ ($i = 1$ and 2) coordinates of the two camera stations (exterior orientation elements).

However, these parameters are linearly dependent in the collinearity equations and, thus, if a linear least-squares adjustment is to be employed to determine coordinates of object points, the equation must first be linearized.

The linearization of the collinearity equation by the Taylor Series yields the following general form:

$$\mathbf{V}_{ij} + \dot{\mathbf{B}}_{ij}\,\dot{\delta}_i + \ddot{\mathbf{B}}_{ij}\,\ddot{\delta}_j = \boldsymbol{\epsilon}_{ij} \tag{1}$$

where $\dot{\mathbf{B}}_{ij}$ = a 2×6 matrix which is the partial derivatives of the collinearity equations with respect to the six parameters; that is,

$$\dot{\mathbf{B}}_{ij} = \begin{bmatrix} \frac{\partial F}{\partial X_i} & \frac{\partial F}{\partial Y_i} & \frac{\partial F}{\partial Z_i} & \frac{\partial F}{\partial \omega_i} & \frac{\partial F}{\partial \phi_i} & \frac{\partial F}{\partial \kappa_i} \\ \frac{\partial G}{\partial X_i} & \frac{\partial G}{\partial Y_i} & \frac{\partial G}{\partial Z_i} & \frac{\partial G}{\partial \omega_i} & \frac{\partial G}{\partial \phi_i} & \frac{\partial G}{\partial \kappa_i} \end{bmatrix}$$

This form may be simply noted as

$$\dot{\mathbf{B}}_{ij} = \begin{bmatrix} a_1 & a_2 & a_3 & a_4 & a_5 & a_6 \\ b_1 & b_2 & b_3 & b_4 & b_5 & b_6 \end{bmatrix}.$$

$\ddot{\mathbf{B}}_{ij}$ = a 2×3 matrix which is the derivatives of the collinearity equations with respect to the X_j, Y_j, Z_j ground coordinates of the j^{th} object point; thus,

$$\ddot{\mathbf{B}}_{ij} = \begin{bmatrix} \frac{\partial F}{\partial X_j} & \frac{\partial F}{\partial Y_j} & \frac{\partial F}{\partial Z_j} \\ \frac{\partial G}{\partial X_j} & \frac{\partial G}{\partial Y_j} & \frac{\partial G}{\partial Z_j} \end{bmatrix} = \begin{bmatrix} a_7 & a_8 & a_9 \\ b_7 & b_8 & b_9 \end{bmatrix}.$$

$\dot{\boldsymbol{\delta}}_i$ = a 6 × 1 vector which consists of the corrections to the approximate values of the parameters used in the linearization. The transpose of this vector is

$$(\dot{\boldsymbol{\delta}}_i)^{T} = [\Delta X_i \; \Delta Y_i \; \Delta Z_i \; \Delta\omega_i \; \Delta\phi_i \; \Delta\kappa_i].$$

$\ddot{\boldsymbol{\delta}}_i$ is a 3 × 1 vector of the corrections to the approximate values of the ground coordinates of the object point, which is in transposed form

$$(\ddot{\boldsymbol{\delta}}_i) = [\Delta X_j \; \Delta Y_j \; \Delta Z_j].$$

$\boldsymbol{\epsilon}_{ij}$ = a 2 × 1 vector which is the differences between the refined photocoordinates and those computed from the F and G functions using approximate values for the parameters and noting them as F_0 and G_0; thus,

$$\boldsymbol{\epsilon}_{ij} = \begin{bmatrix} x_{ij} - F_0 \\ y_{ij} - G_0 \end{bmatrix} \text{ or } \boldsymbol{\epsilon}_{ij} = \begin{bmatrix} a_{10} \\ b_{10} \end{bmatrix}.$$

The $\mathbf{V}_{ij}$ is a 2 × 1 vector of the residuals of the photocoordinates, i.e.,

$$\mathbf{V}_{ij} = \begin{bmatrix} v_{x_{ij}} \\ v_{y_{ij}} \end{bmatrix}.$$

practical technique for large blocks whereby the system is reduced with $\dot{\boldsymbol{\delta}}$ vector being treated first followed by the solution of the individual $\ddot{\boldsymbol{\delta}}$ subvectors one at a time, as demonstrated by Brown (1974, 1976).

The following notation can be used to demonstrate the composition of submatrices in a normal equation:

$$\dot{\mathbf{N}} = \dot{\mathbf{B}}^{T}\mathbf{W}\dot{\mathbf{B}}$$
$$\ddot{\mathbf{N}} = \ddot{\mathbf{B}}^{T}\mathbf{W}\ddot{\mathbf{B}}$$
$$\bar{\mathbf{N}} = \ddot{\mathbf{B}}^{T}\mathbf{W}\dot{\mathbf{B}}$$
$$\dot{\mathbf{c}} = \dot{\mathbf{B}}^{T}\mathbf{W}\boldsymbol{\epsilon}$$
$$\ddot{\mathbf{c}} = \ddot{\mathbf{B}}^{T}\mathbf{W}\boldsymbol{\epsilon}$$

$\dot{\boldsymbol{\epsilon}}$ = $6n$ × 1 vector of discrepancies between a priori values of elements of exterior orientation and the corresponding values used in linearization of a collinearity equation.

$\ddot{\boldsymbol{\epsilon}}$ = $3m$ × 1 vector of discrepancies between a priori values of coordinates of measured ground points and corresponding values used in linearization of the collinearity equation.

Then the normal equation, as composed of submatrices, is

$$\begin{bmatrix}
\ddot{\mathbf{N}}_1 + \ddot{\mathbf{W}}_1 & 0 & \cdots & 0 & \bar{\mathbf{N}}_{11} & \bar{\mathbf{N}}_{12} & \cdots & \bar{\mathbf{N}}_{1n} \\
0 & \ddot{\mathbf{N}}_2 + \ddot{\mathbf{W}}_2 & \cdots & 0 & \bar{\mathbf{N}}_{21} & \bar{\mathbf{N}}_{21} & & \bar{\mathbf{N}}_{1n} \\
\vdots & \vdots & & \vdots & \vdots & \vdots & & \vdots \\
0 & 0 & \cdots & \ddot{\mathbf{N}}_m + \ddot{\mathbf{W}}_m & \bar{\mathbf{N}}_{m1} & \bar{\mathbf{N}}_{m2} & \cdots & \bar{\mathbf{N}}_{mn} \\
\bar{\mathbf{N}}_{11}^{T} & \bar{\mathbf{N}}_{21}^{T} & & \bar{\mathbf{N}}_{m1}^{T} & \dot{\mathbf{N}}_1 + \dot{\mathbf{W}}_1 & 0 & \cdots & 0 \\
\bar{\mathbf{N}}_{12}^{T} & \bar{\mathbf{N}}_{22}^{T} & & \bar{\mathbf{N}}_{m2}^{T} & 0 & \dot{\mathbf{N}}_2 + \dot{\mathbf{W}}_2 & \cdots & 0 \\
\vdots & \vdots & & \vdots & \vdots & \vdots & & \vdots \\
\bar{\mathbf{N}}_{1n}^{T} & \bar{\mathbf{N}}_{2n}^{T} & \cdots & \bar{\mathbf{N}}_{mn}^{T} & 0 & 0 & \cdots & \dot{\mathbf{N}}_n + \dot{\mathbf{W}}_n
\end{bmatrix}
\begin{bmatrix} \ddot{\boldsymbol{\delta}}_1 \\ \ddot{\boldsymbol{\delta}}_2 \\ \vdots \\ \ddot{\boldsymbol{\delta}}_m \\ \dot{\boldsymbol{\delta}}_1 \\ \dot{\boldsymbol{\delta}}_2 \\ \vdots \\ \dot{\boldsymbol{\delta}}_n \end{bmatrix}
=
\begin{bmatrix} \ddot{\mathbf{c}}_1 - \ddot{\mathbf{W}}_1\ddot{\boldsymbol{\epsilon}}_1 \\ \ddot{\mathbf{c}}_2 - \ddot{\mathbf{W}}_2\ddot{\boldsymbol{\epsilon}}_2 \\ \vdots \\ \ddot{\mathbf{c}}_m - \ddot{\mathbf{W}}_m\ddot{\boldsymbol{\epsilon}}_m \\ \dot{\mathbf{c}}_1 - \dot{\mathbf{W}}_1\dot{\boldsymbol{\epsilon}}_1 \\ \dot{\mathbf{c}}_2 - \dot{\mathbf{W}}_2\dot{\boldsymbol{\epsilon}}_2 \\ \vdots \\ \dot{\mathbf{c}}_n - \dot{\mathbf{W}}_n\dot{\boldsymbol{\epsilon}}_n \end{bmatrix}
\quad (3)$$

If the weights of the observed photo-coordinates are noted as $\mathbf{W}$, the normal equation matrix may be obtained as:

$$\begin{bmatrix} \ddot{\mathbf{B}}^{T}\mathbf{W}\ddot{\mathbf{B}} + \ddot{\mathbf{W}} & \ddot{\mathbf{B}}^{T}\mathbf{W}\dot{\mathbf{B}} \\ \dot{\mathbf{B}}^{T}\mathbf{W}\ddot{\mathbf{B}} & \dot{\mathbf{B}}^{T}\mathbf{W}\dot{\mathbf{B}} + \dot{\mathbf{W}} \end{bmatrix} \begin{bmatrix} \ddot{\boldsymbol{\delta}} \\ \dot{\boldsymbol{\delta}} \end{bmatrix} = \begin{bmatrix} \ddot{\mathbf{B}}^{T}\mathbf{W}\boldsymbol{\epsilon} - \ddot{\mathbf{W}}\ddot{\boldsymbol{\epsilon}} \\ \dot{\mathbf{B}}^{T}\mathbf{W}\boldsymbol{\epsilon} - \dot{\mathbf{W}}\dot{\boldsymbol{\epsilon}} \end{bmatrix} \quad (2)$$

where $\dot{\mathbf{W}}$ is the inverse variance-covariance matrix of the a priori estimates of the camera exterior orientation elements, and $\ddot{\mathbf{W}}$ is the inverse variance-covariance matrix of the a priori estimates of ground coordinates.

The normal equations can either be solved simultaneously for all parameters, or by a more

The optimization of the computation depends on the way the normal equations are formed and solved. For photogrammetric monitoring six camera stations (n = 6) and 100 target points were (m = 100) found to be sufficient. The maximum size of a normal equation is $(6n + 3m)^2 = 112896$. The system, therefore, must be economized.

A matrix form of the linearized set of observation equations for the j^{th} point on the i^{th} photograph is shown by Equation 1 from which normal equations are directly formed. The organization of an observation equation coefficient is shown by Figure 1.

Each equation (for x or y) is divided by the stan-

$$
\begin{array}{llllll}
a_1a_1 \\
a_1a_2 & a_2a_2 \\
a_1a_3 & a_2a_3 & a_3a_3 \\
a_1a_4 & a_2a_4 & a_3a_4 & a_4a_4 \\
a_1a_5 & a_2a_5 & a_3a_5 & a_4a_5 & a_5a_5 \\
a_1a_6 & a_2a_6 & a_3a_6 & a_4a_6 & a_5a_6 & a_6a_6
\end{array}
$$

21 elements of $\dot{N}_i$ (group I)

$$
\begin{array}{llllll}
a_1a_7 & a_2a_7 & a_3a_7 & a_4a_7 & a_5a_7 & a_6a_7 \\
a_1a_8 & a_2a_8 & a_3a_8 & a_4a_8 & a_5a_8 & a_6a_8 \\
a_1a_9 & a_2a_9 & a_3a_9 & a_4a_9 & a_5a_9 & a_6a_9
\end{array}
$$

18 elements of $\bar{N}_{ij}$ (group II)

$$
\begin{array}{lll}
a_7a_7 \\
a_7a_8 & a_8a_8 \\
a_7a_9 & a_8a_9 & a_9a_9
\end{array}
$$

6 elements of $\ddot{N}_j$ (group III)

$$
\begin{array}{llllll}
a_1a_{10} & a_2a_{10} & a_3a_{10} & a_4a_{10} & a_5a_{10} & a_6a_{10}
\end{array}
$$

6 elements of $\dot{c}_i$ (group IV)

$$
\begin{array}{lll}
a_7a_{10} & a_8a_{10} & a_9a_{10}
\end{array}
$$

3 elements of $\ddot{c}_j$ (group V)

FIG. 1. Organization of normalized values obtained from an observation equation of the x coordinate. These values are ready to be directly accumulated into the initialized locations of the normal equations.

dard error of a particular observation and then the coefficients (a_k, $k = 1, 2, \ldots, 10$) are multiplied in pairs. Thus, 54 individual products are obtained as shown by Figure 1 for the i[th] photograph and the j[th] ground point. The $\mathbf{N}_i$ submatrix of Equation 3 is obtained from group I, the values of $\bar{\mathbf{N}}_{ij}$ from group II, the values of $\ddot{\mathbf{N}}_j$ from group III, and the values of $\dot{\mathbf{c}}_i$ and $\ddot{\mathbf{c}}_j$ from groups IV and V, respectively. A similar procedure can be followed by using the b_k coefficient.

Normal equations, therefore, are obtained by accumulation using one observation equation at a time.

Normal equation submatrices are stored separately in symmetric storage mode ignoring the null submatrices. In this way the maximum elements of a normal equation are 11,526. Normal equations are solved by inverting the submatrices one at a time using the Cholesky's matrix inversion.

The terms in the $\dot{\boldsymbol{\delta}}$ and $\ddot{\boldsymbol{\delta}}$ vectors are obtained and their standard errors are computed from the following equations:

$$
\begin{aligned}
\sigma_{\dot{\delta}} &= \sqrt{\sigma^2{}_0\, q_{11}} \\
\sigma_{\ddot{\delta}} &= \sqrt{\sigma^2{}_0\, q_{xx}}
\end{aligned}
\tag{4}
$$

where the unit variance is computed from

$$
\sigma^2{}_0 = \frac{\mathbf{V}^{\mathrm{T}}\mathbf{W}\mathbf{V} + \dot{\boldsymbol{\epsilon}}^{\mathrm{T}}\mathbf{W}\boldsymbol{\epsilon} + \ddot{\boldsymbol{\epsilon}}^{\mathrm{T}}\ddot{\mathbf{W}}\ddot{\boldsymbol{\epsilon}}}{\text{Degrees of Freedom}}
$$

and q_{11} and q_{xx} are the diagonal elements of the $\mathbf{Q}_{LL}$ and $\mathbf{Q}_{xx}$ matrices, which are

$$
\begin{aligned}
\mathbf{Q}_{LL} &= \left[(\dot{\mathbf{N}} + \dot{\mathbf{W}}) - \bar{\mathbf{N}}(\ddot{\mathbf{N}} + \ddot{\mathbf{W}})^{-1}\,\bar{\mathbf{N}}^{\mathrm{T}}\right]^{-1} \\
\mathbf{Q}_{xx} &= (\ddot{\mathbf{N}} + \ddot{\mathbf{W}}) + \mathbf{P}\mathbf{Q}_{LL}\mathbf{P}^{\mathrm{T}} \\
\mathbf{P} &= (\ddot{\mathbf{N}} + \ddot{\mathbf{W}})^{-1}\,\bar{\mathbf{N}}^{\mathrm{T}}.
\end{aligned}
$$

The method is an iterative process and the last iteration is determined when the vectors $\dot{\boldsymbol{\delta}}$, $\ddot{\boldsymbol{\delta}}$ are nearly equal to zero. The standard errors and residuals provide an opportunity for a statistical analysis and elimination of blunders. The output of the sequential adjustment is analyzed in terms of residuals of coordinates of intersected points. Large residuals result in large a posteriori variances. If an intersected point is obtained from more than two images, the one with the highest residual error is removed after the appropriate statistical test. This eliminates the blunders from the a priori values of simultaneous adjustment. The last iteration provides a posteriori values of the simultaneous adjustment which should not be significantly different from the a priori's assumed weight σ_{ui}, a hypothesis test $H_{\alpha i}$ is performed (Uotila, 1975). The $H_{\alpha i}$ hypothesis is there's a blunder in the i^{th} observation if

$$
\frac{U_i}{u_i} > F_1^{1/2}, \infty, 1 - \alpha_0
$$

In the present case, the significant level α_0 is assumed as 0.05. The F distribution function is taken from tables as a function of α_0, β_0, where β_0 is assumed as 80 percent.

A substantial practical advantage of a simultaneous adjustment is secured by the fact that a minimum seven fixed parameters are required for the computation. Therefore, if permanent terrestrial camera stations are established, as is desirable for long range monitoring, the field control measurements are reduced to a minimum. The first camera station provides six parameters, namely, the three coordinates of the frontal nodal point of the camera and three orientation angles. The seventh parameter is the X coordinate of the second camera station. Thus, the only ground measurement required is the base line between the two camera stations.

SIMULATED MODEL AND PRACTICAL EXPERIMENTS

The purpose of a simulated experiment is to determine the proper geometry and design standards for variable geometric combinations of aerial and terrestrial photographs. Also, the effect of different computer generated errors was studied.

A simulated experiment consists of a mathematical test area which has been selected to express a generalized surface. This hypothetical test area has dimensions of 2000 by 2000 feet and incorporated 99 points. Fictitious photographs are established by computing errorless image points using Equation 1.

The geometry of a photogrammetric survey can be expressed in terms of parallactic angles. The term terrestrial parallactic angle (*Pt*) expresses the angle of intersection between the optical axes of two terrestrial cameras at the center of the plane containing the targets. The parallactic angle for an aerial camera (*Pa*) is defined as the angle between the axis of an aerial camera and a horizontal plane. Three terrestrial parallactic angles were selected; namely, 30°, 60°, and 90° in connection with aerial parallactic angles of 30°, 60°, and 82°, resulting in a total of twelve combinations.

Computer generated errors were introduced to the fictitious image coordinates which consisted of

- Round off errors (the generated image coordinates were rounded off to the nearest micrometre);
- Systematic errors in terms of residuals from lens distortion correction function, film shrinkage, and atmospheric refraction; and
- Random errors to a magnitude of six micrometres.

The standard errors σ_X, σ_Y, σ_Z of the coordinates of ground points were computed from the simultaneous adjustment (Equation 4). The position error of each point is obtained from the following equation:

$$\sigma_p = \pm \sqrt{\sigma_X^2 + \sigma_Y^2 + \sigma_Z^2}$$

A desirable geometry and design criterion was based on the position error as a function of the two parallactic angles. It is recognized that position error is a function of several variables; however, it was simplified by incorporating only the parallactic angles in order to arrive at a convenient design criterion.

The obtained results are illustrated in graph form by Figure 2. It can be interpreted from the graph that, if the terrestrial parallactic angle is larger than 60° and combined with an aerial parallactic angle of larger than 30°, an excellent geometry and accuracy can be achieved. Terrestrial parallactic angles close to 30° provide a weak geometry; thus, this should be avoided. It can be emphasized, in general, that the role of an aerial photograph is very important as it increases obtainable accuracy from 20 percent up to 50 percent. It may be noted that an aerial parallactic angle close to 90° provides an undefined solution. Thus, aerial photographs utilized for this purpose must deviate at least 5° from the vertical.

Practical experiments were performed on the Gabion Wall which is part of the Interstate 90 Highway system in Washington State. Its description is given in detail by Veress and Sun (1978) and Veress and Hatzopoulos (1979). There are a large number of terrestrial photographs of the wall available. Thus, the comparison between terrestrial photogrammetric monitoring and the combined aerial and terrestrial photogrammetric monitoring becomes possible.

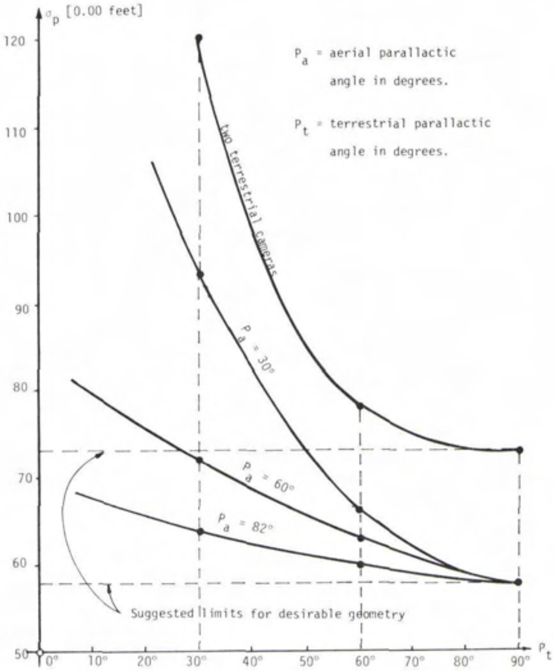

FIG. 2. Analysis of the position error effect by introducing all types of error to the image coordinates.

For this research, the combination of aerial and terrestrial photographs was obtained on 27 October 1976, 12 April 1977, 19 September 1978, and 14 May 1979. They were used for practical experiments. The Wild RC5/RC8 aerial camera with f = 152 mm and an average resolution of 52 line pairs per millimetre was used for photographing on 27 October 1976 and 12 April 1977. The aerial camera (a modified Aero/View 600 with a Fairchild Ericon lens of f = 152 mm) was used for photographing on 19 September 1978 and 14 May 1979. They were calibrated for this purpose by the United States Geological Survey with an average resolution of 61 line pairs per millimetre. The Wild camera was mounted on the floor of the airplane in a typical mapping position and the plane was rotated during photography. The Aero/View camera was mounted on a rotating platform on the floor of the airplane with a view of the Gabion wall through the removed aircraft door.

The terrestrial camera was a KA-2 (f = 610 mm) modified for 23 by 23 cm glass plates. It was calibrated by the United States Geological Survey at the Reston Office. The measurements were performed on the negative photographic plates or film.

The terrestrial photographs were taken approximately at a 3,200 foot photographic distance and the aerial photographs were obtained approximately at a 1,500 foot altitude above the structure.

The terrestrial photographs covered all the targets, but only 45 percent were imaged on the aerial photographs of 27 October 1976, 39 percent on 12 April 1977, 20 percent on 19 September 1978, and 75 percent on 14 May 1979. The quality of the photographs varied because of the weather conditions during which they were taken.

The following average standard errors were obtained from the simultaneous adjustment:

27 October 1976
$\sigma_x = \pm 5$ mm $\sigma_y = \pm 4$ mm $\sigma_z = \pm 12$ mm

12 April 1977
$\sigma_x = \pm 4$ mm $\sigma_y = \pm 3$ mm $\sigma_z = \pm 6$ mm

19 September 1978
$\sigma_x = \pm 6$ mm $\sigma_y = \pm 5$ mm $\sigma_z = \pm 21$ mm

14 May 1979
$\sigma_x = \pm 6$ mm $\sigma_y = \pm 6$ mm $\sigma_z = \pm 10$ mm

ANALYSIS OF RESULTS

The combination of aerial and terrestrial photographs for structural monitoring or other precise photogrammetric surveys can be performed with both sequential and simultaneous computations. The various errors introduced in the simulation experiments indicated that the largest effect on the sequential adjustment is the error in the coordinates of the principal point of the photograph, while the effect of this error is much smaller on the simultaneous adjustment (the maximum was about 20 μm). The changes in the front nodal point coordinates due to this error is considerably larger than that of the simultaneous adjustment, which absorbed this error more uniformly by the exterior orientation elements. The simultaneous adjustment provides better results under all assumed errors if a precise well calibrated camera is available. When a small gross error exists in the observation, the sequential method is less influenced by this error than the simultaneous adjustment.

The simulation as well as the practical experiments indicated that the inclusion of aerial photographs substantially increased the obtainable accuracy. The practical experiments were made under a large variation of conditions.

The photograph taken at the number one camera station on 14 May 1979 was not measurable, due to damaged negative. Consequently, there were differences in number of camera stations used in computation. The quality of the aerial photographs varied not just because two cameras were used but also because of the variable weather conditions.

The obtained relative accuracy is close to that predicted by the simulation experiments. The maximum improvement is in the vertical direction representing a 40 percent improvement as compared to the data obtained from terrestrial photographs alone.

The established criteria for the design of such a project proved to be adequate for practical photogrammetric surveys. The terrestrial photographs exhibited a greater sensitivity for the parallactic angle than the combination of aerial and terrestrial images.

These experiments in general indicate that the utilization of such a survey is feasible from a theoretical and practical point of view.

The opinions, findings, and conclusions expressed in this publication are those of the author and are not necessarily those of the Washington State Department of Transportation or of the Federal Highway Administration.

References

Bauer, H., and J. Muller, 1972. *Height Accuracy of Blocks and Bundle Adjustment with Additional Parameters,* Presented Paper of Commission III, ISP Congress, Ottawa.

Brandenberger, A. J., and M. T. Erez, 1972. Photogrammetric Determination of Displacements and Deformations in Large Engineering Structures, *The Canadian Surveyor,* Vol. 26, No. 2.

Brown, D. C., 1974. Bundle Adjustment with Strip-and-Block-Invariant Parameters, *Bul,* Vol. 42, No. 6, pp. 210-220, 1974.

———, 1976. *The Bundle Adjustment-Progress and Prospects,* Invited Paper, Commission III, XIII Congress of ISP, Helsinki.

Erlandson, J. P., and S. A. Veress, 1975. Monitoring Deformations of Structures, *Photogrammetric Engineering and Remote Sensing,* Vol. 41, No. 11, pp. 1375-1384.

———, 1976. Photogrammetrische Erfassung von Bauwerksveranderungen, *VR-Vermessugswesen und Raumordnung,* Heft 8.

Fraser, C. S., 1979. *Simultaneous Multiple Camera and Multiple Focal Setting Self-Calibration in Photogrammetry,* Dissertation, University of Washington. 1979b.

Gutu, A., 1972. A Photogrammetric Measurement Accuracy of Wall Pillar Cracks in Rock Salt Mines, *Buletin de Fotogrammetrie, Special Issue.*

Hatzopoulos, J. N., *Combination of Aerial and Terrestrial Photogrammetry in Structural Monitoring,* Dissertation, University of Washington.

Hou, M. C. Y., Water Dam Control Surveying and Adjustments, *Proceedings of the ACSM, 39th Annual Meeting, Washington D. C.,* March 18-24.

Kenefick, J. F., 1971. Ultra-Precise Analysis, *Photogrammetric Engineering,* Vol. 37, No. 11, pp. 1167-1187.

Planicka, A., 1970. *Die Renutzung der Terrestrischen Photogrammetrie in Deformationsmessung von Steinschuttdammen,* Paper presented at the 6th Internal Course for Engineering Surveys of High Precision, Graz, Austria.

Schmid, H. H., 1956. An Analytical Treatment of the Problem of Triangulation by Stereophotogrammetry, *Photogrammetria,* pp. 67-77 and 91-116.

Uotila, U. A., 1975. Statistical Tests as Guidelines in

Analysis of Adjustment of Control Nets, *Surveying and Mapping,* ACSM, pp. 47-52.

Veress, S. A., 1971. *Determination of Motion and Deflection of Retaining Walls,* Part I, Theoretical Considerations, University of Washingtaon, Final Technical Report. 1971.

———, 1980a. Photogrammetry for Dimensional Control of Bridges, *International Archives of Photogrammetry,* Vol. 5, pp. 746-755.

———, 1980b. Contemporary Analytical Solution in Terrestrial Photogrammetry, *International Archives of Photogrammetry,* Vol. 10, pp. 164-174.

Veress, S. A., and G. E. De Gross, 1971. *Determination of Motion and Deflection of Retaining Walls,* Part II, Technical Applications, University of Washington, Final Technical Report.

Veress, S. A., J. P. Erlandson, and J. C. Peterson, 1973. *Performance of Observations of Structural Deformations by Photogrammetric Methods, Technical Report, U.S. Army Corps of Engineers, Seattle District.*

Veress, S. A., and J. N. Hatzopoulos, 1979. *Monitoring by Aerial and Terrestrial Photogrammetry,* Final Technical Report, Washington State Dept. of Transportation WA-RD-38.1.

Veress, S. A., M. C. Y., Hou, E. E. Flint, L. L. Sun, J. N. Hatzopoulos, and C. Jijina, 1977. *Photogrammetric Monitoring of a Gabion Wall,* Final Technical Report, Department of Transportation, Report No. 31.1, Research Project Y-1699.

Veress, S. A., N. G. Jackson, and J. N. Hatzopoulos, 1980. Monitoring of a Gabion Wall by Inclinometer and Photogrammetry, *Photogrammetric Engineering and Remote Sensing,* Vol. 46, No. 6, pp. 771-778.

Veress, S. A., and L. L. Sun, 1978. Photogrammetric Monitoring of a Gabion Wall, *Photogrammetric Engineering and Remote Sensing,* Vol. 44, No. 2, pp. 205-211.

(Received 3 November 1980; revised and accepted 15 May 1981)